Pyrolysis biochar systems, balance between bioenergy and carbon sequestration

GLOBAL CHANGE BIOLOGY
BIOENERGY

GCB Bioenergy (2014), doi: 10.1111/gcbb.12137

Pyrolysis biochar systems, balance between bioenergy and carbon sequestration

KYLE CROMBIE and ONDŘEJ MAŠEK

UK Biochar Research Centre, School of GeoSciences, University of Edinburgh, Crew Building, King's Buildings, Edinburgh EH9 3JN, UK

Abstract

This study aimed to investigate the extent to which it is possible to marry the two seemingly opposing concepts of heat and/or power production from biomass with carbon sequestration in the form of biochar. To do this, we investigated the effects of feedstock, highest heating temperature (HTT), residence time at HTT and carrier gas flow rate on the distribution of pyrolysis co-products and their energy content, as well as the carbon sequestration potential of biochar. Biochar was produced from wood pellets (WP) and straw pellets (SP) at two temperatures (350 and 650 °C), with three residence times (10, 20 and 40 min) and three carrier gas flow rates (0, 0.33 and 0.66 l min^{-1}). The energy balance of the system was determined experimentally by quantifying the energy contained within pyrolysis co-products. Biochar was also analysed for physicochemical and soil functional properties, namely environmentally stable-C and labile-C content. Residence time showed no considerable effect on any of the measured properties. Increased HTT resulted in higher concentrations of fixed C, total C and stable-C in biochar, as well as higher heating value (HHV) due to the increased release of volatile compounds. Increased carrier gas flow rate resulted in decreased biochar yields and reduced biochar stable-C and labile-C content. Pyrolysis at 650 °C showed an increased stable-C yield as well as a decreased proportion of energy stored in the biochar fraction but increased stored energy in the liquid and gas co-products. Carrier gas flow rate was also seen to be influential in determining the proportion of energy stored in the gas phase. Understanding the influence of production conditions on long term biochar stability in addition to the energy content of the co-products obtained from pyrolysis is critical for the development of specifically engineered biochar, be it for agricultural use, carbon storage, energy generation or combinations of the three.

Keywords: biochar, carbon sequestration, energy balance, higher heating value, labile carbon, physicochemical properties, pyrolysis, stable carbon

Received 2 August 2013 and accepted 6 September 2013

Introduction

Global climate change and the inevitable depletion of fossil fuel reserves are among the major challenges facing humanity in the 21st century, which has led to a boom in research related to alternative energy sources and reducing greenhouse gas (GHG) emissions. With global production of biomass estimated at >147 billion tons per year it can be regarded as a renewable energy source with the largest potential to contribute to global energy demands (Balat & Ayar, 2005; Bridgwater, 2006; Demirbas, 2007). Biomass has the potential to produce renewable sources of liquid, gaseous and solid fuels while also offering a route for long-term carbon storage. The energy contained within biomass can be extracted by different thermo-chemical or biological methods, including fermentation, direct combustion, gasification, pyrolysis etc.

Correspondence: Ondrej Masek, tel. + 0131 6505095, fax + 0131 6620478, e-mail: ondrej.masek@ed.ac.uk

Pyrolysis is the thermo-chemical conversion of biomass in an oxygen-depleted environment at temperatures above ca. 300 °C. Under these conditions organic materials decompose to non-condensable gases, condensable organic liquids and a carbonaceous solid (biochar). As all of these are potentially valuable co-products, biomass pyrolysis is a polygeneration technology, which offers more than one product, and is thus a highly efficient process for biomass conversion (Demirbas, 2007; Chen *et al*., 2012; Song & Guo, 2012).

Although biochar has high energy content, in many cases, its more beneficial application is incorporation into soil to increase the long-term storage of carbon, while also providing soil amendment benefits and greenhouse gas reduction (Shackley & Sohi, 2010; Sohi *et al*., 2010). The mechanisms by which biochar influences soil fertility are not yet fully understood, but literature shows that biochar can have a significant impact on soil organic carbon, water holding capacity, cation exchange capacity, pH and soil microbial ecology

(Sohi *et al*., 2010; Ronsse *et al*., 2013). Biochar can be considered to be part of the black carbon continuum used to characterize the carbon products of combustion and through 14C dating has been found to display mean residence times of several thousand years (Masiello, 2004; Preston & Schmidt, 2006; Lehmann *et al*., 2009).

The liquid product obtained from pyrolysis, known as bio-oil, is a result of rapid and simultaneous depolymerizing and fragmentation reactions of the three main components of biomass: cellulose, hemicellulose and lignin. Bio-oil composition is therefore strongly linked to the composition of the initial feedstock. Bio-oil tends to have a high concentration of oxygen (45–50%) and differs greatly from petroleum fuels (Mohan *et al*., 2006). Bio-oil consists of two (sometimes three) phases, first, a non-aqueous phase consisting of insoluble high molecular weight organics (tar) and second, an aqueous phase containing low molecular weight organo-oxygen compounds (Demirbas, 2007). Bio-oil is a complex mixture of over 300 compounds including acids, aldehydes, ketones, sugars, phenols etc., and can serve as a precursor for synthesis of many other chemicals (Demirbas, 2007; Thangalazhy-Gopakumar *et al*., 2010). Bio-oil can also be used as a replacement for fossil fuels in boilers, furnaces and, after some treatment and/or engine modifications, in engines for heat and power generation (Boerrigter & Rauch, 2005; Bridgwater, 2012).

The mixture of non-condensable gases produced during pyrolysis consists mainly of CO_2, CO, CH_4, H_2 and C_2 hydrocarbons. As with the liquid fraction, the gas product can be utilized for heat and power generation in combustion turbines and engines, however, the most common application is for providing heat to sustain the pyrolysis process and to dry biomass feedstock (Becidan *et al*., 2007). The selection of pyrolysis production conditions such as feedstock, moisture content, temperature, heating rate etc. affects the final yield and composition of the gas, liquid and solid products while also influencing the properties and energy content of these products. The co-production of solid char, liquid bio-oil and pyrolysis gas can improve the efficiency of biomass conversion in different socio-economic contexts, as opposed to a system designed to maximize only one single product (Chen *et al*., 2012).

Due to the numerous important differences between different pyrolysis processes (temperature, heating rate, vapour residence time etc.) and the large variety of potentially available biomass and other organic feedstock for pyrolysis, it is clear that there can be an almost infinite number of different biochars produced, differing in physicochemical properties and performance as a soil amendment (Enders *et al*., 2012; Ronsse *et al*., 2013). However, little has been reported on the effect of production conditions on the combination of functional properties of biochar and energy balance of the system. Functional properties can be regarded as properties which influence the response and effect of biochar in soil such as stability, labile-C content, nutrient availability etc. Maximizing the yield of biochar for agricultural application and therefore carbon sequestration potential of biochar has long been associated with decreasing the severity of pyrolysis, resulting in a loss of energy as a result of reduced liquid and gas fractions (Antal & Grønli, 2003; Demirbas, 2004; Demiral & Ayan, 2011; Hossain *et al*., 2011; Angin, 2012; Chen *et al*., 2012; Manyà, 2012; Crombie *et al*., 2013; Mašek *et al*., 2013; Ronsse *et al*., 2013). Biochar production therefore faces competition for resources from alternative technologies such as fast pyrolysis and gasification, which are largely focused on maximizing the extraction of energy rich liquid and gas products while generating very small amounts of char (<15%) (Bridgwater, 2012). However, very little is actually known about the influence of production conditions on the product energy distribution and at the same time the carbon sequestration potential of biochar.

Determining how the pyrolysis conditions relate to biochar functional properties and energy generation is pivotal to assess biochar's potential role in sequestering carbon and offsetting carbon emissions, as well as to provide environmental services. This study therefore aims to show the influence that feedstock and production conditions has on the amount of carbon and energy stored in biochar, as well as the amount of available energy in pyrolysis liquids and gas. This should then indicate whether and under what circumstances it may be possible to simultaneously achieve high efficiency of biomass conversion into heat and/or power and high carbon sequestration potential.

Materials and methods

Feedstock

The two types of biomass used for the pyrolysis experiments were: mixed 5/95 pine : spruce softwood pellets (WP) and mixed 50/50 wheat : oilseed rape straw pellets (SP) with respective moisture content measured at 10.6% for WP and 5.4% for SP (gravimetrically loss on drying at 105 °C for 24 h). WP (ø 6 mm) was acquired from Puffin Pellets, Aberdeenshire, Scotland while SP (ø 6 mm) was acquired from StrawPellet Ltd., Rookery Farm, Lincolnshire, England. All feedstock was used as received with good homogeneity for pellet material. Results from ultimate and proximate analysis of the selected materials are shown in Table 1.

Table 1 Proximate and ultimate analysis for straw and wood pellet feedstock

	Proximate analysis [wt.% (db)]			Ultimate analysis [wt.% (db)]						
Sample	Fixed C%	Volatile matter%	Ash%	C%	H%	N%	O%	O : C	H : C	HHV [MJ kg^{-1}]
Straw pellet feed	15.3	77.2	7.4	42.0	5.5	0.1	44.9	0.8	1.6	15.8
Wood pellet feed	17.2	77.2	5.7	53.7	6.7	0.0	33.9	0.5	1.5	17.6

Equipment

A detailed description of the equipment type and set-up can be found in Crombie *et al.* (2013). The pyrolysis equipment used for sample production, shown in Fig. 1, consists of a fixed bed reactor made of a vertical quartz tube (50 mm d) with sintered plate at the base allowing a sample bed depth of up to ca. 200 mm. The sample in the reactor tube was heated by a 12 k W infrared gold image furnace (P610C; ULVAC-RIKO, Yokohama, Japan) with a proportional–integral–derivative controller allowing a wide range of heating rates and hold times with possible HTT over 1000 °C. Before each experiment, the glassware apparatus was assembled and the system was purged with nitrogen (N_2). Before starting the heating, the N_2 flow rate was adjusted to the desired level. The N_2 gas was used to sweep volatiles and gases away from the pyrolysis zone and into the condensation system. The condenser system consisted of three stages, a high temperature zone (at 160 °C) for condensation of heavy tar components, an ambient temperature zone for collection of water and water soluble organic compounds, and a low temperature (−40 °C) zone consisting of two traps for capture of light aromatics. All the remaining noncondensable gases were collected in a 200 l multi-layered gas bag (JensenInert Products, Coral Springs, Florida). When the end of the desired residence time has been reached the samples were gradual cooled (with continued N_2 flow) until below 100 °C (about 1 h.) and removed for storage in a sealed container.

Pyrolysis conditions

Pyrolysis experiments used a standard mass (100 g for WP and SP) of feedstock, resulting in a different volume of material being used in runs due to different feedstock density. The WP and SP feedstock were selected for investigating the effect of highest treatment temperature (HTT), residence time at HTT and carrier gas flow rate on the energy content of pyrolysis

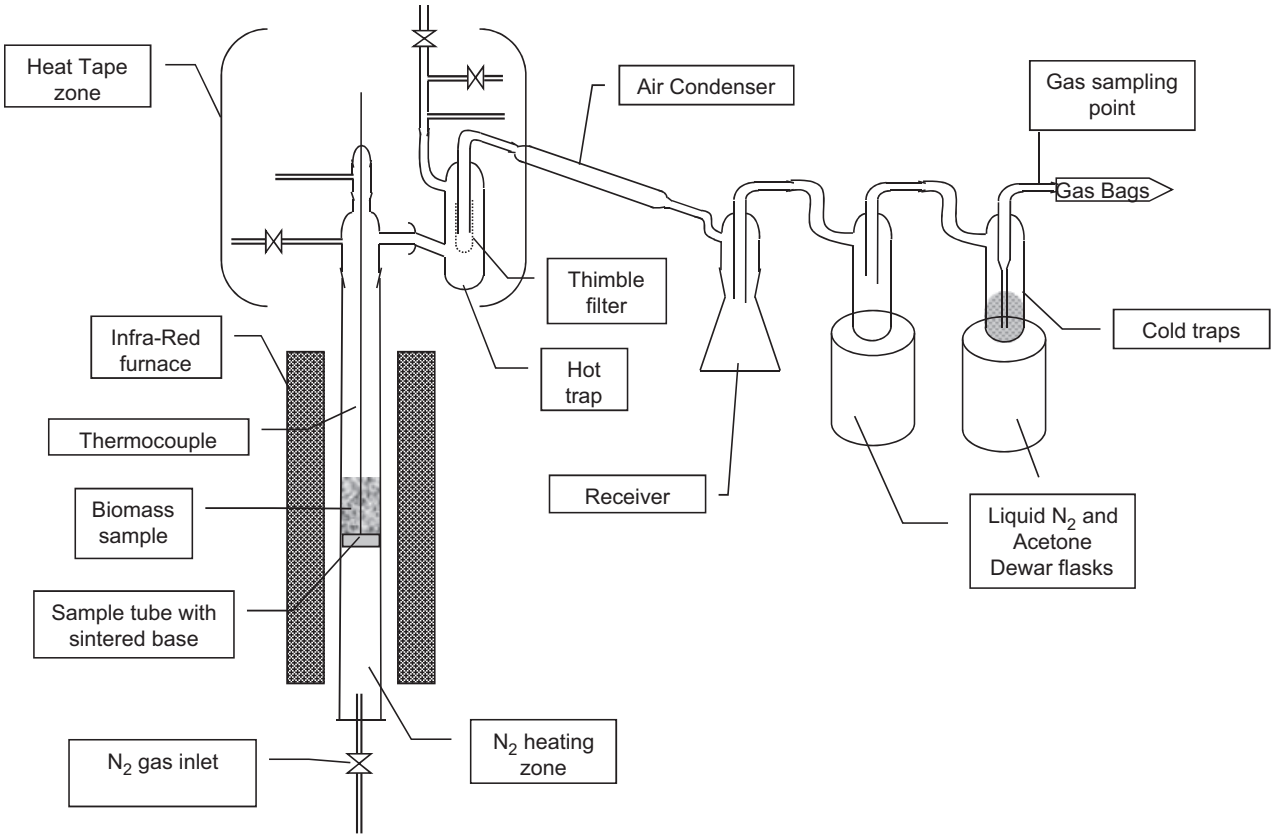

Fig. 1 Small scale batch pyrolysis unit located at UKBRC.

products. Samples of both feedstock types were heated at a rate of 5 °C min^{-1}. The WP and SP runs were implemented using HTT of 350 °C and 650 °C. These two temperatures were selected to generate samples of biochar representing both the lower and higher end of temperatures used for biochar production, and to provide considerably different product distributions. The holding times at HTT (residence time) of 10, 20 and 40 min were selected so that they represented realistic residence times in industrial continuous pyrolysis units. The carrier gas flow rates were altered between 0, 0.33 and 0.66 l min^{-1} to provide sufficient range to assess the importance of this parameter on biomass pyrolysis. After pyrolysis, the different products were collected, measured and stored as described in Crombie *et al*. (2013).

Product analysis

Biochar physicochemical analysis. Biochar samples were crushed to a homogenous fine powder and dried overnight at 105 °C prior to proximate and ultimate analysis. Proximate analysis of all biochar samples and corresponding feedstock was carried out using thermo gravimetric analysis (Mettler-Toledo TGA/DSC1, UKBRC, Edinburgh, UK). Samples were first heated for 10 min at 105 °C under N_2 to determine moisture content; the temperature was then raised at 25 °C min^{-1} to 900 °C where it remained for further 10 min to eliminate volatile matter. With air introduced to the system the sample is finally combusted (also at 900 °C) for 20 min to determine ash. Fixed C was calculated on a weight per cent basis by subtracting moisture, volatile and ash values from the original mass. Ultimate analysis of C, H and N was conducted in duplicate using an elemental analyser (Flash 2000, CE Elantech Inc, New Jersey, USA) by London Metropolitan University (London, UK). The O content was determined by difference.

Biochar soil functional analysis. One of the main attractions of biochar is its ability to store atmospheric carbon in soil for hundreds to thousands of years. Real-time experiments to quantify this stability over decades are not feasible, leading to the need for rapid screening tools which could be used to analyse biochar samples and assess their carbon sequestration potential. Therefore, this analysis focused on two key properties of biochar related to its function in soil, namely biochar carbon stability (stable-C%) and content of labile carbon (labile-C%) using analytical techniques developed at UK Biochar Research Centre, as detailed in Cross & Sohi (2011, 2013). In brief, the carbon stability was assessed through accelerated oxidative ageing by treating finely milled biochar (0.1 g C) with 7 ml of 5% hydrogen peroxide, initially at room temperature then 80 °C for 48 h. The content of labile carbon was determined by CO_2 evolution following the incubation of biochar (1 g) in sand (9.5 g) inoculated with a community of soil microbes for a period of 2 weeks at 30 °C.

Higher heating value analysis. To determine the distribution of energy among the pyrolysis products the higher heating value (HHV) of biochar, liquid and gas products was determined analytically. The following section explains the analysis steps for each product in brief.

Biochar higher heating value analysis. Biochar samples were analysed for HHV (in duplicate) using an adiabatic bomb Calorimeter PAR 1261 (accuracy of + 0.1% on two determinations) at Pemberton Analytical Services, Shawbury, Shropshire, UK.

Liquid higher heating value analysis. Liquid samples were separated from the gas stream through a series of condensation traps as shown in Fig. 1. This led to the collection of three different liquid fractions consisting of heavy tars, light liquids condensed at room temperature and finally liquids collected from the first cold trap. For analytical purposes, subsamples of these three fractions were then added together to create one representative liquid sample. The calorific analysis of liquid samples was carried out at the University of York using an isoperibol oxygen bomb calorimeter model Parr 6200. The liquids were treated with a solvent (dodecane) to dissolve the different fractions and also to overcome the difficulty of igniting liquids with high moisture contents. The energy value of the solvent (44.15 kJ g^{-1}) was then subtracted from the total to determine the HHV for the pyrolysis liquid fraction. Duplicate samples were prepared for two SP and WP samples to test the variation in the analysis procedure, and this method confirmed good reproducibility.

Gas higher heating value analysis. Gas samples were collected during each pyrolysis run using 200 l multilayer gas bags. The gas bags were then left to rest for 30 min to allow the mixture to equilibrate after which the overall composition of the collected gas sample was analysed for N_2, H_2, CO, CO_2, CH_4, C_2H_6, O_2 and Ar using a mass spectrometer (HPR-20 QIC, Hiden Analytical, Warrignton, UK). The overall composition of the pyrolysis gas mixture was then used in conjunction with the volume of gas collected and higher heating value of the measured gas species to calculate the HHV of the product gas. Final composition of the pyrolysis gas was corrected for the dilution effect of carrier gas (N_2).

Statistical analysis

Analysis of variance (ANOVA) statistical test was applied through a general linear model using Minitab 16 statistical software and significance of results were calculated at a significance level of $P < 0.05$ for all materials and production conditions. Correlations were performed using Spearman rank method and R values were categorized by considering correlation coefficients < 0.35 to represent low or weak correlations, 0.36–0.67 to be moderate correlations, 0.68–0.90 strong or high correlations and >0.9 to be a very high correlation (Taylor, 1990).

Results

It should be noted that where residence time had no statistically significant influence on the properties of

interest an average value was taken for the obtained results to aid in the representation of feedstock, HTT and carrier gas flow rate influence. Presentation of the results in this way may lead to visual exaggeration of trends but statistical analysis was carried out on the entire data set rather than the average values.

Product distribution

The yields obtained for char, liquid and gas products from each pyrolysis experiment are shown in Fig. 2. For each feedstock, increasing the pyrolysis HTT from 350 °C to 650 °C resulted in a decreased char yield and subsequent increase in the yields of liquids and gases. The distribution of the liquid and gas fraction was largely dependent ($P < 0.0001$) on feedstock composition, thus potentially resulting in the varying yields and properties between the two biomass types (Vassilev *et al*., 2010; Crombie *et al*., 2013). However, the influence of feedstock on char yield only became significant when in conjunction with HTT ($P < 0.05$). The resulting change in product yields with temperature is due to increasing decomposition of cellulose, hemicellulose and lignin at elevated HTT causing increased emissions of volatile matter ($R^2 = -0.9$, $P < 0.0001$) (Enders *et al*., 2012; Crombie *et al*., 2013). WP demonstrated the largest variation between biochar yields as well as the highest (55%) and lowest (27%) char yields at 350 °C and 650 °C respectively. There was a smaller variation observed between SP biochar samples at different HTT. With increasing release of volatile matter the yields of liquid and gas products could be expected to continue to rise with HTT, however, there was a substantially larger increase in the yield of pyrolysis gas compared to that of liquids. This is likely due to secondary cracking reactions converting liquid volatiles into gas around 500 °C (Chen *et al*., 2003; Phan *et al*., 2008; Duman *et al*., 2011; Fu *et al*., 2011).

In this study the residence time at HTT had no statistically significant effects on the char, liquid and gas yields ($P = 0.23$, $P = 0.36$ and $P = 0.79$ respectively). Increasing the range of residence times investigated may generate more obvious trends or significant differences in values. However, the range used in this study was chosen to correspond to realistic times for biochar production in industrial continuous pyrolysis units.

Reducing the vapour residence time could have a direct effect on the composition of liquid and gaseous products obtained from the pyrolysis system by affecting the interactions of the volatile matter with char and other gaseous species. The results in Fig. 2 show, that although the effect of the carrier gas flow rate on the char, liquid and gas yields (when analysing the full data set) is not as clear as that of temperature, it is still significant ($P < 0.05$). Pyrolysis of WP in the absence of a carrier gas generated the highest char yields (>50%) compared to the other carrier gas flow rates used (<45%). As there was no carrier flow the expelled volatile matter was propelled through the system only by the action of gas produced during pyrolysis. Therefore, these conditions would encourage secondary char formation by interaction of char and volatiles, which could explain the higher char and lower liquid and gas yields. When investigating further it was found that carrier gas flow rate had a significant effect on the liquid yields at 350 °C; however, no impact was observed at 650 °C ($P = 0.41$) potentially due to the maximum liquid yield being reached at ca. 500 °C (Chen *et al*., 2003; Phan *et al*., 2008; Duman *et al*., 2011).

Physicochemical properties

The influence of production conditions on the results obtained from proximate and ultimate analysis is important for quantitative assessment of the composition of biochar as well as an indication of its stability.

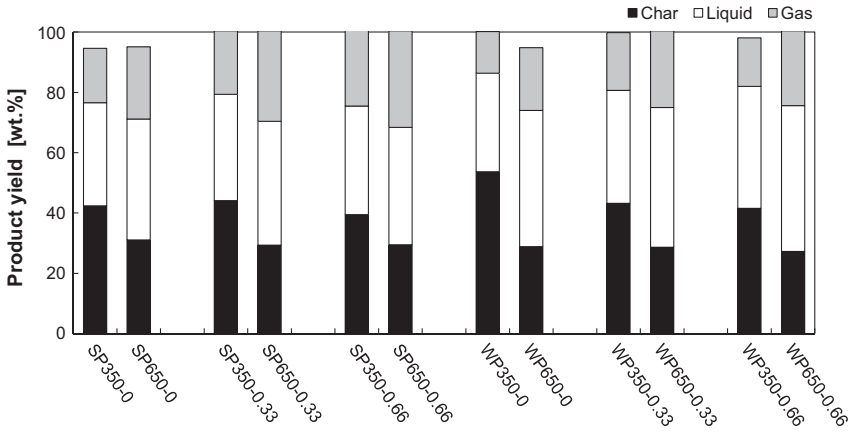

Fig. 2 Slow pyrolysis product distribution.

However, as these results were not the primary focus of this study, a detailed analysis can be found in Data S1, and only a brief description of the main trends will be provided in the following section.

Proximate analysis

Results for proximate analysis of all char samples are shown in Table 2. The measured ash content varied greatly between feedstock ($P < 0.0001$) with higher concentrations found in biochar derived from SP (12–23%) biomass compared to WP biochar (<3%). Higher HTT promoted biomass decomposition, leading to higher fixed C and reduced volatile matter concentrations in the resulting biochar. Similar trends were also exhibited by the corresponding fixed C and volatile matter yields. Carrier gas flow rate and residence time at HTT were both found to have no significant effect ($P > 0.05$) on the composition of biochar, as determined by proximate analysis.

Ultimate analysis

Data from ultimate analysis (Table 2) showed preferential release of H and O, and retention of C, with increasing HTT for both types of feedstock and all residence times and carrier gas flow rates. As seen with fixed C, there appeared to be a significant influence ($P < 0.05$) of

Table 2 Proximate and ultimate analysis for all biochar samples

	Proximate analysis [wt.% (db)]					Ultimate analysis [wt.% (db)]				
Sample	Fixed C	Volatile matter	Ash	FC yield (daf)	VM yield (daf)	C	H	N	O	C Yield
SP 350-10-0	45.8	39.2	15.0	33.1	28.3	61.4	3.6	1.0	19.0	61.4
SP 350-20-0	45.6	39.1	15.3	33.8	29.0	62.7	4.4	1.1	16.5	62.8
SP 350-40-0	39.5	38.8	21.7	29.3	28.8	56.6	2.9	1.1	17.6	58.0
SP 650-10-0	59.2	19.9	20.9	40.9	13.7	71.1	1.3	1.0	5.8	54.6
SP 650-20-0	57.5	19.6	22.9	39.3	13.4	72.1	1.3	0.9	2.8	52.8
SP 650-40-0	62.9	16.2	20.9	41.6	10.7	73.2	1.2	1.1	3.5	52.4
SP 350-10-0.3	36.7	51.0	12.3	27.6	38.3	55.5	4.2	0.9	27.1	65.9
SP 350-20-0.3	40.0	45.9	14.2	30.3	34.7	60.4	5.2	1.1	19.2	65.0
SP 350-40-0.3	46.8	37.0	16.2	30.8	24.3	62.1	3.0	1.0	17.8	55.1
SP 650-10-0.3	58.3	20.4	21.4	36.5	12.8	69.2	1.2	1.0	7.2	49.3
SP 650-20-0.3	62.2	17.7	20.1	38.8	11.0	71.2	1.0	1.0	6.7	49.9
SP 650-40-0.3	59.3	19.0	21.8	37.0	11.8	71.4	1.1	1.2	4.6	48.8
SP 350-10-0.6	44.2	40.6	15.2	32.0	29.4	62.0	4.7	1.1	16.9	61.4
SP 350-20-0.6	47.1	36.9	16.0	33.1	25.9	62.9	4.6	1.1	15.4	59.0
SP 350-40-0.6	50.4	33.0	16.6	34.7	22.7	64.6	4.3	1.1	13.4	57.3
SP 650-10-0.6	59.4	20.0	20.5	38.1	12.8	71.8	1.6	1.0	5.1	50.9
SP 650-20-0.6	56.1	22.5	21.4	35.8	14.4	68.8	1.4	1.1	7.4	50.2
SP 650-40-0.6	61.8	16.2	22.0	38.3	10.0	72.5	1.3	1.1	3.0	48.4
WP 350-10-0	48.6	50.7	0.8	34.2	35.7	67.3	4.5	0.0	27.5	69.9
WP 350-20-0	50.8	48.0	1.2	33.2	31.4	63.5	5.3	0.1	30.0	64.6
WP 350-40-0	54.5	44.2	1.2	35.6	28.8	68.4	4.6	0.0	25.8	64.4
WP 650-10-0	90.5	8.1	1.4	44.7	4.0	90.4	2.2	0.1	5.9	48.8
WP 650-20-0	90.4	7.5	2.1	43.8	3.6	89.8	2.2	0.1	5.9	47.5
WP 650-40-0	91.3	6.7	2.0	45.1	3.3	90.0	2.0	0.1	5.9	48.5
WP 350-10-0.3	57.9	40.7	1.4	33.4	23.5	71.4	4.5	0.0	22.7	56.9
WP 350-20-0.3	56.4	42.4	1.2	31.8	24.0	70.6	5.5	0.1	22.6	55.8
WP 350-40-0.3	60.2	38.4	1.4	36.1	23.0	71.4	4.5	0.0	22.7	59.1
WP 650-10-0.3	89.0	8.8	2.2	44.9	4.5	92.8	1.7	0.0	3.3	49.3
WP 650-20-0.3	88.5	8.8	2.8	43.2	4.3	87.9	2.1	0.1	7.2	47.5
WP 650-40-0.3	89.4	9.1	1.5	43.1	4.4	90.2	1.8	0.0	6.4	47.5
WP 350-10-0.6	54.6	44.1	1.2	32.4	26.2	70.1	5.1	0.1	23.4	58.6
WP 350-20-0.6	65.7	33.0	1.3	37.3	18.8	76.4	5.0	0.1	17.2	56.1
WP 350-40-0.6	55.9	42.6	1.5	28.7	21.9	67.4	5.9	0.1	25.2	50.6
WP 650-10-0.6	89.0	9.5	1.5	41.7	4.5	90.2	1.8	0.0	6.5	46.2
WP 650-20-0.6	89.2	9.1	1.8	40.1	4.1	87.1	1.8	0.0	9.3	44.2
WP 650-40-0.6	89.1	9.7	1.2	39.8	4.3	87.4	1.8	0.0	9.6	44.1

feedstock on the total biochar C content, with the high ash SP biochar containing a lower amount of C compared to WP biochar at corresponding temperatures. As with fixed-C content, there was no significant effect of the residence time or carrier gas flow rate on C content at either of the two HTTs used. However, as with feedstock selection, the carrier gas flow rate did show an effect on the C yield obtained at 350 °C.

Biochar elemental ratios of O : C and H : C were used to construct a Van Krevelen diagram (Fig. 3), typically used as a visual representation of the age/maturity and origin of hydrocarbon materials such as coal and petroleum. There was a distinct separation between low and high temperature biochar with 650 °C char being classified as highly stable according to criteria proposed by Spokas (Spokas, 2010), IBI Guidelines (IBI Guidelines, 2012) and European biochar guidelines (Schmidt *et al*., 2012). At 650 °C, all biochar samples contained O : C ratio of <0.08 indicating high stability while the spread of O:C values for 350 °C ranged from 0.16 to 0.37 for SP and from 0.17 to 0.36 for WP.

Soil functional properties of biochar

The following section will present the results of two analytical tools, developed by the UKBRC (Cross & Sohi, 2011, 2013), and how production conditions may impact the carbon storage potential of biochar. Residence times used at both HTT had no significant influence ($P > 0.6$) on the stable-C and labile-C content of biochar and therefore will not be discussed further, although the data will be used in place of replicates to examine effects of other parameters. The error bars used in Figs 4 and 5 represent the three replicates done at the same HTT and carrier gas flow rate, but different holding time.

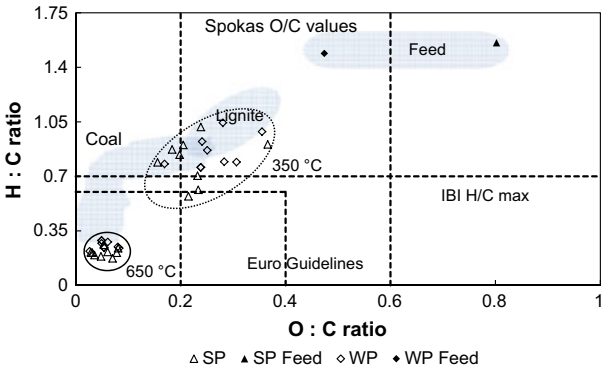

Fig. 3 Van Krevelen diagram indicating the stability of SP and WP biochar.

Carbon stability (Edinburgh stability tool)

Results for stable-C content (on biochar C basis) and stable-C yield (on feedstock C basis), determined by the direct oxidation method, are plotted in Fig. 4. It can be seen that temperature was the main factor influencing the concentration and yield of stable carbon, with higher HTT resulting in much higher biochar stability ($P < 0.0001$) and higher proportion of feedstock carbon being locked in the form of a stable biochar carbon. The

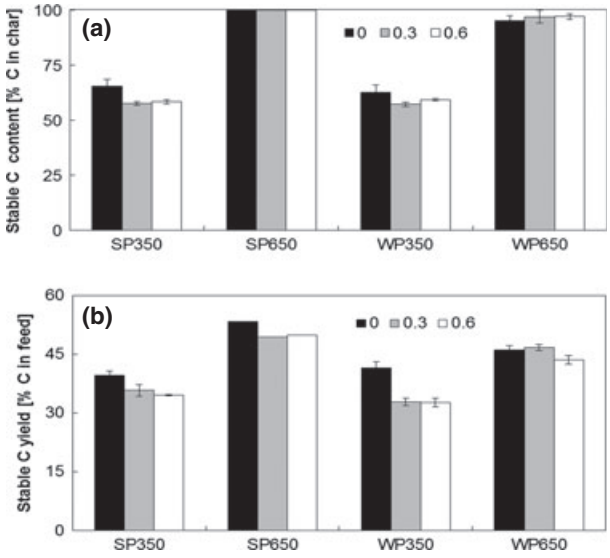

Fig. 4 Environmental stability of SP and WP char expressed on (a) char carbon basis, (b) feedstock carbon basis.

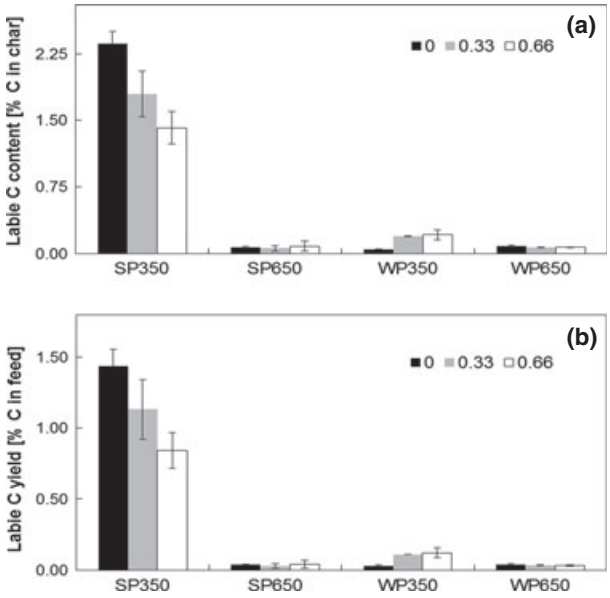

Fig. 5 Labile-C content of SP and WP biochar expressed on (a) char carbon basis, (b) feedstock carbon basis.

stable-C content range at 350 °C was 57–65% while a HTT of 650 °C raised these values to 95–100%.

Besides the HTT, the carrier gas (N_2) flow rate also had an important effect on stable-C content and yield. With decreasing carrier gas flow rate the stability and yield of stable-C increased, especially at low HTT. This can be explained by devolatilization of char particles, resulting in enhanced formation of secondary char within and on the surface of biochar. Although the effect of carrier gas flow rate was only secondary to that of HTT, our results show that it is an important parameter influencing biochar yield and properties. On the other hand, feedstock showed only minimal if any effect ($P > 0.05$) on the stable-C content of chars produced at low HTT (350 °C) and slight, but statistically significant ($P < 0.05$) effect at high HTT (650 °C). Expressing results on a feedstock C basis (stable-C yield) provides a useful way of assessing the efficiency of feedstock C conversion into stable-C that can be sequestered in the form of biochar. Results in Fig. 4 show that although the biochar yield (wt.%) was greatly reduced as temperature was increased there was still an overall increase in stable-C yield from 350 °C to 650 °C.

Labile carbon (Edinburgh labile-C tool)

The content of labile carbon, defined as carbon readily accessible to soil microbes, is mainly affected by the HTT and feedstock, as shown in Fig. 5. With increasing HTT from 350 °C to 650 °C, the content of labile carbon in biochar dropped dramatically to levels below 0.1 wt.%. Feedstock type was also shown to be an important factor in determining labile-C content, at least at low HTT. Pyrolysis of SP at 350 °C resulted in char with much higher labile-C content (1.86 ± 0.29%) than that produced by pyrolysis of WP (0.15 ± 0.05%). The influence of feedstock decreased with pyrolysis HTT, resulting in no significant effect ($P > 0.05$) at 650 °C due to the dominant impact of temperature. The carrier gas flow rate was found to have no significant effect ($P > 0.65$) on the final labile-C content or labile-C yield obtained at either HTT (Fig. 5).

Heating value of pyrolysis co-products

The higher heating value (HHV) data for solid, liquid and gas products obtained from each experiment are presented in Table 3. The following section discusses the relative distribution of energy among the three co-products of slow pyrolysis and how it is affected by process parameters.

The HHV for each biochar sample was seen to increase with higher HTT with a larger increase occurring for WP biochar. This is due to the fact that with increasing pyrolysis severity the char composition shifts closer towards pure carbon with HHV of 32.8 MJ kg^{-1} (Ronsse *et al.*, 2013). Ronsse *et al.* (2013) also suggested that the presence of ash in the char can lead to a 'dilution' of the energy content resulting in lower than pure carbon HHV for fully carbonized materials. The lower HHV for SP chars produced at 650 °C could be explained by this 'dilution' effect as a result of the increasing ash concentration with temperature and the higher ash content of SP chars compared to WP. Alternatively, the presence of C-H, C-O and O-H bonds remaining in the char have been seen to influence the HHV of biochar, in particular wood derived biochar has been shown to produce HHV higher than pure carbon (up to 35 MJ kg^{-1}) (Ronsse *et al.*, 2013). However, the HHV of wood materials may in fact peak and then decline as the heterogeneous bonding is sequentially decreased following stabilization of the carbon structure (Ronsse *et al.*, 2013). Temperature clearly had the largest influence ($P < 0.0001$) on the char HHV with carrier gas flow rate ($P = 0.003$) and feedstock ($P < 0.0001$) also having a significant impact. However, the effect of carrier gas flow rate on the char heating value was only observed at 350 °C with no effect seen at 650 °C ($P > 0.05$). The observed trend of biochar HHV can then be used to further emphasize the dominance of temperature on biochar properties at 650 °C. Residence time had no significant influence ($P > 0.75$) on the HHV of biochar at either HTT.

The HHV for the liquid samples produced during each experimental run was unaffected by increases in HTT, residence time and carrier gas flow rate ($P > 0.5$). Therefore, the difference in liquid HHV was mainly derived from feedstock composition ($P = 0.002$) with the average liquid heating values for SP and WP measured as 7.24 ± 0.2 MJ Kg^{-1} and 6.20 ± 0.21 MJ Kg^{-1} respectively. Biochar ash concentration and HHV of liquids did show a moderate correlation ($R^2 = 0.46$, $P = 0.005$) indicating the small difference between SP and WP liquid HHV could be related to the increased ash concentration of SP biomass.

The higher heating value (HHV) of pyrolysis gas was calculated based on the gas composition as shown in shown in Fig. 6. It can be seen that the pyrolysis gas HHV increases considerably with increasing HTT, as a result of increased concentrations of H_2, CH_4, C_2H_6 and CO measured in the pyrolysis gas. The increase in these species could be a result of aromatic condensation and secondary thermal cracking of heavy hydrocarbons occurring above 550 °C (Chen *et al.*, 2003, 2012; Mohan *et al.*, 2006; Yang *et al.*, 2006; Duman *et al.*, 2011; Fu *et al.*, 2011). The release of CO_2 and CO is predominantly associated with the cracking and reforming of carbonyl, ether groups and thermolabile carboxyl while

Table 3 Higher heating value (HHV) for solid, liquid and gas co-products obtained from slow pyrolysis

	Higher Heating Value of Pyrolysis Co-products					
Sample	Char HHV (MJ kg^{-1})	Liquid HHV (MJ kg^{-1})	Gas HHV (MJ kg^{-1})	Energy contained in Char (MJ)	Energy contained in Liquid (MJ)	Energy contained in Gas (MJ)
SP 350-10-0	24.1	7.8	3.2	10.1	2.7	0.5
SP 350-20-0	23.1	7.1	3.2	9.7	2.5	0.6
SP 350-40-0	23.8	7.4	3.3	10.3	2.4	0.6
SP 650-10-0	24.0	7.2	9.7	7.7	2.9	2.0
SP 650-20-0	23.0	8.2	9.7	7.1	3.2	2.7
SP 650-40-0	24.4	6.2	11.1	7.3	2.5	2.5
SP 350-10-0.3	21.6	6.4	2.5	10.8	2.0	0.5
SP 350-20-0.3	22.1	8.2	2.8	10.0	2.8	0.7
SP 350-40-0.3	22.3	9.2	3.5	8.3	3.7	0.9
SP 650-10-0.3	24.7	7.3	9.4	7.4	3.0	3.0
SP 650-20-0.3	25.1	6.9	9.5	7.4	2.8	3.0
SP 650-40-0.3	23.5	6.3	7.8	6.8	2.6	2.5
SP 350-10-0.6	24.6	6.3	3.9	10.2	2.1	1.0
SP 350-20-0.6	24.6	7.1	4.3	9.7	2.6	1.1
SP 350-40-0.6	24.3	6.4	4.7	9.1	2.4	1.3
SP 650-10-0.6	24.8	7.1	9.4	7.4	2.8	3.3
SP 650-20-0.6	24.1	7.2	9.3	7.4	2.8	3.0
SP 650-40-0.6	25.9	8.3	9.8	7.2	3.2	3.6
WP 350-10-0	27.7	5.3	2.3	15.5	1.7	0.3
WP 350-20-0	26.7	8.2	2.0	14.6	2.8	0.3
WP 350-40-0	27.6	5.6	2.1	13.9	1.8	0.3
WP 650-10-0	33.6	6.6	9.8	9.7	2.9	2.1
WP 650-20-0	33.6	5.7	8.9	9.6	2.7	1.9
WP 650-40-0	33.9	6.8	10.6	9.8	3.0	2.1
WP 350-10-0.3	27.6	6.5	3.1	11.8	2.5	0.6
WP 350-20-0.3	27.8	6.4	3.0	11.8	2.4	0.6
WP 350-40-0.3	27.1	6.2	3.3	12.0	2.3	0.6
WP 650-10-0.3	33.3	5.2	6.0	9.5	2.4	1.7
WP 650-20-0.3	33.2	4.8	8.1	9.6	2.2	2.0
WP 650-40-0.3	33.1	6.5	8.0	9.4	3.0	2.0
WP 350-10-0.6	27.7	6.1	4.8	12.5	2.3	0.8
WP 350-20-0.6	28.7	4.6	5.1	11.3	1.9	0.8
WP 350-40-0.6	28.9	6.6	4.5	11.7	2.8	0.7
WP 650-10-0.6	33.7	6.1	11.4	9.3	2.9	2.8
WP 650-20-0.6	33.7	7.4	12.2	9.2	3.6	3.1
WP 650-40-0.6	33.4	6.9	12.8	9.1	3.3	3.4

CO can also be formed through the secondary decomposition of volatiles at higher temperatures (Yang *et al*., 2006; Fu *et al*., 2011). The cracking and reforming of aromatic rings has been described as a pathway for the formation of H_2 as well as the formation of CH_4 through the rupture of methylene groups (Chen *et al*., 2003; Yang *et al*., 2006; Wang *et al*., 2009; Fu *et al*., 2011). Feedstock and residence time were deemed to have no influence ($P > 0.45$) on the pyrolysis gas HHV, while carrier gas flow rate had a significant effect ($P < 0.0001$). Concentrations of H_2, CH_4 and C_2H_6 increased with a higher carrier gas flow rate resulting in increased pyrolysis gas HHV. The resulting increase in HHV was also generated by diminishing CO_2 content with HTT and carrier gas flow rate. This was probably due to the decreased vapour residence time allowing for energy rich species to be swept away from hot char surfaces minimizing secondary reactions.

Energy distribution among co-products

The contribution of each co-product to the overall energy balance was determined by expressing the co-product energy content as a proportion of the feedstock energy content. There was no considerable effect of residence time on the energy distribution among the different product fractions so an average of the values for the different residence times was calculated to

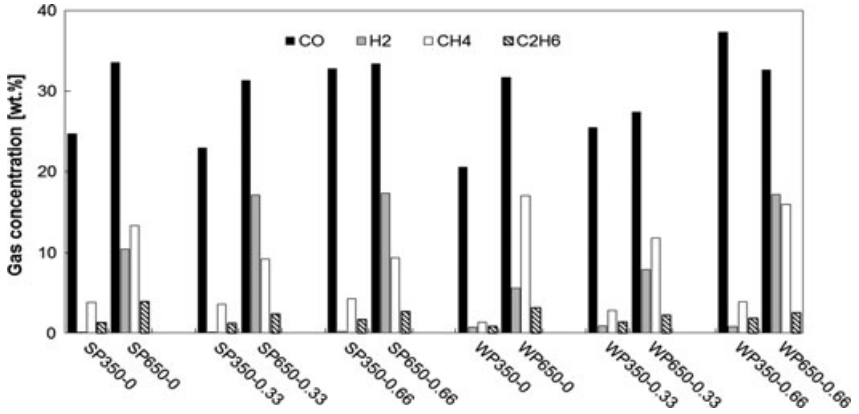

Fig. 6 Effect of temperature and carrier gas flow rate on the gas composition.

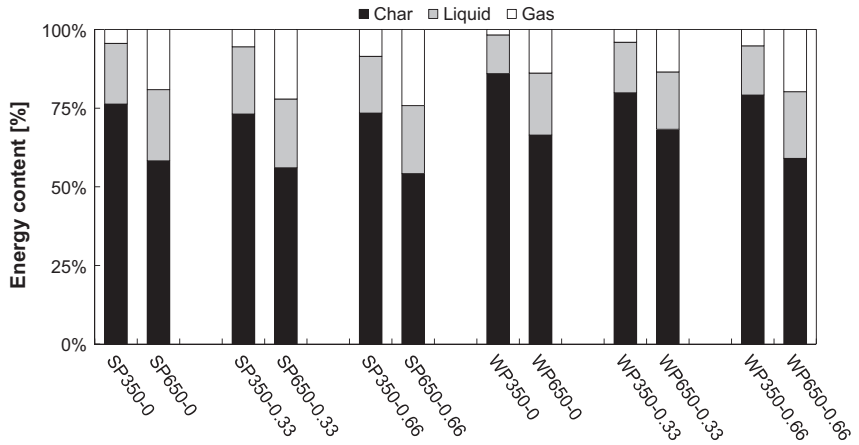

Fig. 7 Normalized energy content distribution among char, liquid and gas co-products.

demonstrate the influence of HTT and carrier gas flow rate on the energy balance (Fig. 7).

As the HTT was increased, biochar showed a significant ($P < 0.0001$) decrease in its contribution to the total energy balance of 15.8 ± 0.47% for SP and 18.9 ± 6.57% for WP material (Fig. 7). The degree of reduction in the biochar contribution was smaller for SP biochar samples, perhaps, due to dilution effect of ash content on biochar HHV. The HHV of the individual liquid samples did not show an increase with HTT but the overall liquid yield and therefore liquid contribution to total energy balance did ($P = 0.003$). Increasing the HTT from 350 °C to 650 °C increased the liquid contribution to total energy from 2.43 ± 0.26 MJ kg^{-1} to 2.88 ± 0.19 MJ kg^{-1}, which represents 2.56% and 2.85% of the total energy recovered in pyrolysis co-products for WP and SP respectively. The contribution of the pyrolysis gas to the total energy balance showed a significant ($P < 0.0001$) increase with higher HTT, due to increased gas yield as well as substantially higher gas HHV at 650 °C. Similarly increasing the carrier gas flow rate also resulted in a significant increase ($P < 0.0001$) in the gas energy contribution to total energy balance, as a result of higher gas yields obtained at higher carrier gas flow rates. Overall, HTT was the controlling variable in determining the distribution of the total energy among the solid, liquid and gas co-products, however, carrier gas flow rate and feedstock were also determining factors at the lower HTT.

Carbon emissions

A breakdown of the C mass distribution between the char, liquid and gas fractions is shown in Table 4. With rising HTT, increasing amount of C is apportioned to the liquid and gas fractions, at the expense of C in the char. However, as previously shown in Fig. 4, despite the decreasing char C content with rising HTT, the biochar stable-C yield increased and therefore stable-C mass also increased. It is important to note that the stable-C (>100 years) and relatively non-stable labile-C (2 week incubations) do not account for the total C

Table 4 Distribution of carbon among co-products

	C in char			C in liquid C in Gas		Stored C (g)		Emitted C (g)	
Sample	Stable C (g)	Labile C (g)	Int-C (g)	(g)	(g)	With Int-C	W/O Int-C	W/O Int-C	With Int-C
SP350-0	15.5	0.6	7.7	10.1	5.3	23.2	15.5	15.9	23.6
SP650-0	21.1	0.0	0.0	10.0	8.6	21.1	20.0	18.5	18.5
SP350-0.33	14.2	0.5	10.0	8.0	7.1	24.2	14.2	15.5	25.5
SP650-0.33	20.1	0.0	0.0	9.8	10.9	20.1	19.1	20.7	20.7
SP350-0.66	13.9	0.3	9.5	8.2	8.2	23.4	13.9	16.7	26.2
SP650-0.66	19.8	0.0	0.0	8.1	11.8	19.8	18.8	19.9	19.9
WP350-0	20.0	0.0	11.9	12.5	3.7	31.9	20.0	16.2	28.2
WP650-0	22.3	0.0	1.1	18.1	7.0	23.4	22.3	25.1	26.2
WP350-0.33	16.0	0.1	11.9	15.5	5.3	27.9	16.0	20.9	32.8
WP650-0.33	22.8	0.0	0.7	17.1	8.3	23.5	22.8	25.3	26.0
WP350-0.66	16.1	0.1	11.0	17.2	4.9	27.1	16.1	22.2	33.2
WP650-0.66	21.5	0.0	0.6	19.9	7.3	22.1	21.5	27.2	27.8

present in the char, indicating a third fraction of intermediate stability (Sonoyama *et al*., 2006). This additional C fraction (Int-C) can be considered to have intermediate stability (2 weeks < Int-C < 100 years), as it could be rapidly released over a number of years or equally remain stable for decades. Therefore, two values for total mass of emitted C can be calculated for each set of pyrolysis conditions (i) intermediate C considered to be stable and therefore not included in calculation of emitted C; (ii) intermediate C considered to be unstable and therefore included in calculation of emitted C. The significance of the Int-C is much larger at low pyrolysis temperatures, so much so that pyrolysis at 350 °C actually released a higher amount of C than at 650 °C, when the Int-C is deemed to be emitted rather than stored (Fig. 8). There is little to no difference of the Int-C fraction on the amount of C being emitted at higher pyrolysis temperatures due to the majority of remaining biochar C being highly stable. When compared to direct combustion of the biomass feedstock, all pyrolysis experiments produced higher relative emissions. However, the relative emissions for SP at 650 °C were not hugely different to those for biomass combustion, and were considerably lower when the carbon stored in

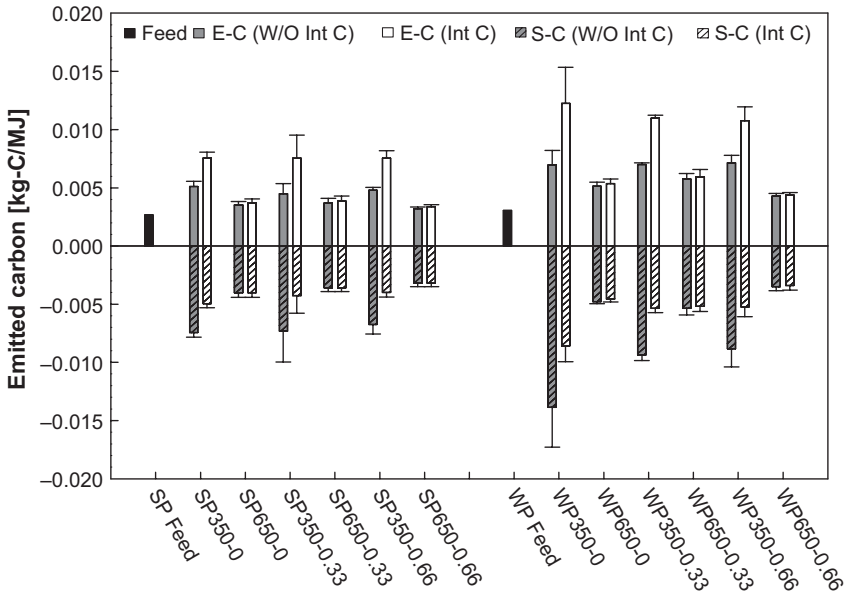

Fig. 8 The effect of temperature and carrier gas flow rate on the amount of stored and emitted C per MJ of chemical energy produced from slow pyrolysis.

biochar was accounted for. This analysis is subject to a number of limitations: first, it works with theoretically available energy in the different material streams, and does not take into account conversion efficiencies of processes potentially utilizing these fuels. Second, it does not include consideration of direct and indirect impacts of biochar on GHG emissions when used in agriculture. These additional benefits can play an important role in overall system-wide carbon balance, and should be included in an LCA, based on the results of this study.

Discussion

Biochar production competes for resources with more established technologies such as fast pyrolysis and gasification that are tuned for electricity or liquid biofuels production and are therefore often heavily subsidized. This focus of utilizing organic feedstock for energy rather than soil amendment or carbon sequestration has led to literature dominated by reports of the composition and heating values of fast pyrolysis products with only a relatively limited number of publications focusing on slow pyrolysis. Therefore, there are gaps in the knowledge needed to fully assess biochar pyrolysis systems and their potential contribution to greenhouse gas management and renewable energy production (Ozcimen & Ersoymericboyu, 2008; Angin, 2012; Gronnow *et al*., 2013; Ronsse *et al*., 2013; Troy *et al*., 2013).

Results of research reported in this article showed that increasing the severity of pyrolysis raised the HHV of the co-products, however, these values on their own do not provide a complete picture of the distribution of energy among co-products; for this the product yield has to be considered. By combining the product yields and HHV the energy distribution between co-products and their resulting heat/power production potential could be evaluated while also assessing any consequential loss of C sequestration potential. It is important to note that the calculated energy balance was based solely on the individual HHV of the collected products and their yields, with no additional consideration of the energy input needed to reach the different temperatures and associated losses, as these are very much process/equipment dependent, and thus presents a first approximation, and important basis for more detailed case studies with detailed LCA, for example, along the lines of (Laird *et al*., 2009; Shackley *et al*., 2011).

Overall, HTT was the controlling variable in determining the distribution of the total energy content among the solid, liquid and gas co-products, however, carrier gas flow rate and feedstock were also determining factors at the lower HTT. Increasing the severity of pyrolysis resulted in a lower contribution of biochar to the overall energy balance, thus reducing the energy potentially lost due to application of biochar to soil. Consequently, the higher HTT increased the energy contained in liquid and gas products that could be associated with increased emissions from the combustion of these products for heat/power production. Therefore, investigating the influence of production conditions on the carbon emissions associated with pyrolysis and use of its products is critical to assessing the environmental as well as energy benefits of high temperature pyrolysis compared to a low temperature one.

By comparing the total energy contained in the liquid and gas fractions with the amount of C emitted by the pyrolysis biochar system, that is, pyrolysis process plus complete combustion of liquids and gases, the relative amounts of stored and emitted C per MJ of chemical energy can be assessed for different combinations of feedstock, HTT and other parameters. In case of pyrolysis at HTT of 350 °C, most of the energy is contained in the char, and therefore unavailable for heat/power generation, while at HTT of 650 °C, most energy is contained in the liquid and gaseous streams. As a result, low temperature pyrolysis releases more C per MJ of energy compared to pyrolysis at 650 °C. Hence, pyrolysis at higher temperatures actually produces fewer emissions per MJ of energy available in the liquid and gaseous co-products, while also securing a larger fraction of C in a stable biochar form.

In summary, higher temperature pyrolysis not only shifted the energy contribution from biochar in favour of the gas and liquid co-products but also led to increased stable-C yields. Therefore, increasing the severity of pyrolysis, at least within the limits investigated, increased the energy value of the pyrolysis gas and liquid fractions, without sacrificing the carbon sequestration potential of biochar. This is an important finding; however, a full life cycle analysis is needed to truly understand all its complex implications. This study presents an important step towards this understanding.

Acknowledgements

This research was supported by a Science and Innovation award from the Engineering and Physical Sciences Research Council in the UK (EP/F017944/1) and laboratory and pyrolysis infrastructure by grants from the Scottish Funding Council and the College of Science and Engineering, University of Edinburgh. Thanks must also be given to Dr Peter Brownsort for his assistance in analysis training.

References

Angin D (2012) Effect of pyrolysis temperature and heating rate on biochar obtained from pyrolysis of safflower seed press cake. *Bioresource Technology*, **128**, 593–597.

Antal MJ, Grønli M (2003) The art, science, and technology of charcoal production †. *Industrial & Engineering Chemistry Research*, **42**, 1619–1640.

Balat M, Ayar G (2005) Biomass energy in the world, use of biomass and potential trends. *Energy Sources*, **27**, 931–940.

Becidan M, Skreiberg Ø, Hustad JE (2007) Products distribution and gas release in pyrolysis of thermally thick biomass residues samples. *Journal of Analytical and Applied Pyrolysis*, **78**, 207–213.

Boerrigter H, Rauch R (2005) Review of applications of gases from biomass gasification. In: *Handbook Biomass Gasification* (eds Knoef HAM), Biomass Technology Group the Netherlands.

Bridgwater A (2006) Biomass for energy. *Biomass*, **1768**, 1755–1768.

Bridgwater AV (2012) Review of fast pyrolysis of biomass and product upgrading. *Biomass and Bioenergy*, **38**, 68–94.

Chen G, Andries J, Luo Z, Spliethoff H (2003) Biomass pyrolysis/gasification for product gas production: the overall investigation of parametric effects. *Energy Conversion and Management*, **44**, 1875–1884.

Chen Y, Yang H, Wang X, Zhang S, Chen H (2012) Biomass-based pyrolytic polygeneration system on cotton stalk pyrolysis: influence of temperature. *Bioresource technology*, **107**, 411–418.

Crombie K, Mašek O, Sohi SP, Brownsort P, Cross A (2013) The effect of pyrolysis conditions on biochar stability as determined by three methods. *GCB Bioenergy*, **5**, 122–131.

Cross A, Sohi SP (2011) The priming potential of biochar products in relation to labile carbon contents and soil organic matter status. *Soil Biology and Biochemistry*, **43**, 2127–2134.

Cross A, Sohi SP (2013) A method for screening the relative long-term stability of biochar. *GCB Bioenergy*, **5**, 215–220.

Demiral I, Ayan EA (2011) Pyrolysis of grape bagasse: effect of pyrolysis conditions on the product yields and characterization of the liquid product. *Bioresource Technology*, **102**, 3946–3951.

Demirbas A (2004) Effects of temperature and particle size on bio-char yield from pyrolysis of agricultural residues. *Journal of Analytical and Applied Pyrolysis*, **72**, 243–248.

Demirbas A (2007) The influence of temperature on the yields of compounds existing in bio-oils obtained from biomass samples via pyrolysis. *Fuel Processing Technology*, **88**, 591–597.

Duman G, Okutucu C, Ucar S, Stahl R, Yanik J (2011) The slow and fast pyrolysis of cherry seed. *Bioresource Technology*, **102**, 1869–1878.

Enders A, Hanley K, Whitman T, Joseph S, Lehmann J (2012) Characterization of biochars to evaluate recalcitrance and agronomic performance. *Bioresource Technology*, **114**, 644–653.

Fu P, Yi W, Bai X, Li Z, Hu S, Xiang J (2011) Effect of temperature on gas composition and char structural features of pyrolyzed agricultural residues. *Bioresource Technology*, **102**, 8211–8219.

Gronnow MJ, Budarin VL, Mašek O *et al.* (2013) Torrefaction/biochar production by microwave and conventional slow pyrolysis - comparison of energy properties. *GCB Bioenergy*, **5**, 144–152.

Hossain MK, Strezov V, Chan KY, Ziolkowski A, Nelson PF (2011) Influence of pyrolysis temperature on production and nutrient properties of wastewater sludge biochar. *Journal of Environmental Management*, **92**, 223–228.

International Biochar Initiative (IBI) Guidelines (2012) Standardized product definition and product testing guidelines for biochar that is used in soil. Available at: http://www.biocharnternational.org/sites/default/files/Guidelines_for_Biochar_That_Is_Used_in_Soil_Final.pdf (accessed 11 October 2013).

Laird D, Brown R, Amonette J, Lehmann J (2009) Review of the pyrolysis platform for coproducing bio-oil and biochar. *Biofuels, Bioproducts and Biorefining*, **3**, 547–562.

Lehmann J, Czimczik C, Laird D, Sohi S (2009) Stability of biochar in soil. In: *Biochar for Environmental Management: Science and Technology* (eds Lehmann J, Joseph S), pp. 183–198. Earthscan, London.

Manyà JJ (2012) Pyrolysis for biochar purposes: a review to establish current knowledge gaps and research needs. *Environmental Science & Technology*, **46**, 7939–7954.

Mašek O, Budarin V, Gronnow M, Crombie K, Brownsort P, Fitzpatrick E, Hurst P (2013) Microwave and slow pyrolysis biochar–comparison of physical and functional properties. *Journal of Analytical and Applied Pyrolysis and Applied Pyrolysis*, **100**, 41–48.

Masiello CA (2004) New directions in black carbon organic geochemistry. *Marine Chemistry*, **92**, 201–213.

Mohan D, Pittman CU, Steele PH (2006) Pyrolysis of wood/biomass for bio-oil: a critical review. *Energy & Fuels*, **20**, 848–889.

Ozcimen D, Ersoymericboyu A (2008) A study on the carbonization of grapeseed and chestnut shell. *Fuel Processing Technology*, **89**, 1041–1046.

Phan AN, Ryu C, Sharifi VN, Swithenbank J (2008) Characterisation of slow pyrolysis products from segregated wastes for energy production. *Journal of Analytical and Applied Pyrolysis*, **81**, 65–71.

Preston CM, Schmidt MWI (2006) Black (pyrogenic) carbon: a synthesis of current knowledge and uncertainties with special consideration of boreal regions. *Biogeosciences*, **3**, 397–420.

Ronsse F, van Hecke S, Dickinson D, Prins W (2013) Production and characterization of slow pyrolysis biochar: influence of feedstock type and pyrolysis conditions. *GCB Bioenergy*, **5**, 104–115.

Schmidt HP, Abiven S, Kammann C, Glaser B, Bucheli T, Leifeld J (2012) *European Biochar Certificate: Guidelines for Biochar Production*. Biochar Science Network, Switzerland.

Shackley S, Sohi S, Brownsort P, *et al.* (2009) *An assessment of the benefits and issues associated with the application of biochar to soil*. A Report Commissioned by the UK Department for Environment, Food and Rural Affairs, and Department of Energy and Climate Change, DEFRA, London.

Shackley S, Hammond J, Gaunt J, Ibarrola R (2011) The feasibility and costs of biochar deployment in the UK. *Carbon Management*, **2**, 335–356.

Sohi S, Krull E, Lopez-Capel E, Bol R (2010) A review of biochar and its use and function in soil. *Advances in Agronomy*, **105**, 47–82.

Song W, Guo M (2012) Quality variations of poultry litter biochar generated at different pyrolysis temperatures. *Journal of Analytical and Applied Pyrolysis*, **94**, 138–145.

Sonoyama N, Okuno T, Mašek O, Hosokai S (2006) Interparticle desorption and re-adsorption of alkali and alkaline earth metallic species within a bed of pyrolyzing char from pulverized woody biomass. *Energy & Fuels*, **20**, 1294–1297.

Spokas K (2010) Review of the stability of biochar in soils: predictability of O: C molar ratios. *Carbon Management*, **1**, 289–303.

Taylor R (1990) Interpretation of the correlation coefficient: a basic review. *Journal of Diagnostic Medical Sonography*, **1**, 35–39.

Thangalazhy-Gopakumar S, Adhikari S, Ravindran H, Gupta RB, Fasina O, Tu M, Fernando SD (2010) Physiochemical properties of bio-oil produced at various temperatures from pine wood using an auger reactor. *Bioresource Technology*, **101**, 8389–8395.

Troy SM, Nolan T, Leahy JJ, Lawlor PG, Healy MG, Kwapinski W (2013) Effect of sawdust addition and composting of feedstock on renewable energy and biochar production from pyrolysis of anaerobically digested pig manure. *Biomass and Bioenergy*, **49**, 1–9.

Vassilev SV, Baxter D, Andersen LK, Vassileva CG (2010) An overview of the chemical composition of biomass. *Fuel*, **89**, 913–933.

Wang S, Wang K, Liu Q, Gu Y, Luo Z, Cen K, Fransson T (2009) Comparison of the pyrolysis behavior of lignins from different tree species. *Biotechnology Advances*, **27**, 562–567.

Yang H, Yan R, Chen H, Zheng C (2006) In-depth investigation of biomass pyrolysis based on three major components: hemicellulose, cellulose and lignin. *Energy & Fuels*, **8**, 388–393.

Supporting Information

Additional Supporting Information may be found in the online version of this article:

Data S1. Proximate analysis.